Electronic Supplementary Material

MoS_2/MnO_2 heterostructured nanodevices for electrochemical energy storage

Xiaobin Liao[1], Yunlong Zhao[1,2], Junhui Wang[1], Wei Yang[1], Lin Xu[1], Xiaocong Tian[1], Yi Shuang[1], Kwadwo Asare Owusu[1], Mengyu Yan[1] (✉), and Liqiang Mai[1,3] (✉)

[1] *State Key Laboratory of Advanced Technology for Materials Synthesis and Processing, Wuhan University of Technology, Wuhan 430070, China*

[2] *Department of Chemistry and Chemical Biology, Harvard University, Cambridge, Massachusetts 02138, USA*

[3] *Department of Chemistry, University of California, Berkeley, California 94720, USA*

Supporting information to https://doi.org/10.1007/s12274-017-1826-6

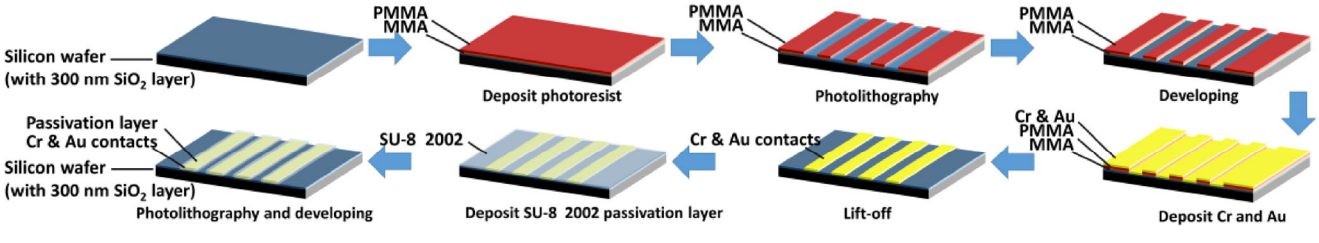

Figure S1 An illustration of the fabrication processes of the energy storage device based on individual heterostructure of MoS_2 nanosheet/MnO_2 nanowire. This process includes the following steps: Step 1, deposited MnO_2 nanowires via spin-coating method on the prepared silicon wafers (with 300 nm SiO_2 layer), and MoS_2 nanosheets obtained through mechanical exfoliation were transferred immediately to the silicon wafer that with MnO_2 nanowires. Then, MMA and PMMA photoresists were coated on silicon wafers with 300 nm SiO_2 layer; Step 2, patterned the metal contacts pad with EBL on silicon wafers; Step 3, developing and rinsing; Step 4, deposited 5 nm Cr and 150 nm Au on to the silicon wafers with thermal evaporation; Step 5, lift-off; Step 6, coated SU-8 2002 on silicon wafers; Step 7, patterned SU-8 2002 with EBL to form the passivation layer that covered the metal contacts, which avoided leakage current.

Address correspondence to Liqiang Mai, mlq518@whut.edu.cn; Mengyu Yan, ymymiles@whut.edu.cn

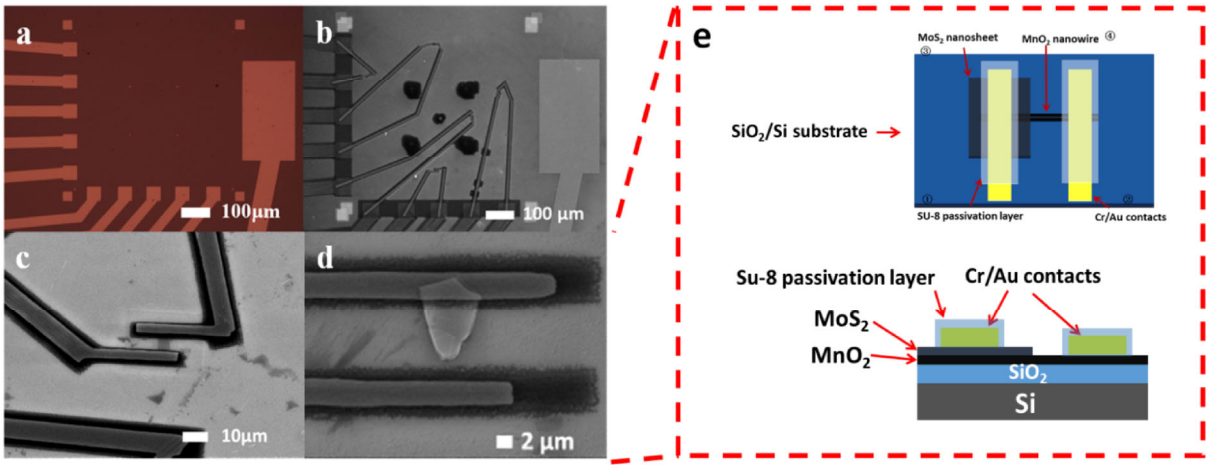

Figure S2 (a) The optical image of the outer electrodes; (b) SEM image of the entail outer electrodes and inner electrodes. The inner electrodes are covered by SU-8 passivation layer to avoid the leakage current; (c) The selected multilayer MoS_2 nanosheet contacts with inner electrodes; (d) SEM image of MoS_2/MnO_2 heterostructure; (e) The illustration of the energy storage device based on individual heterostructure of MoS_2 nanosheet/MnO_2 nanowire in overhead view and front view.

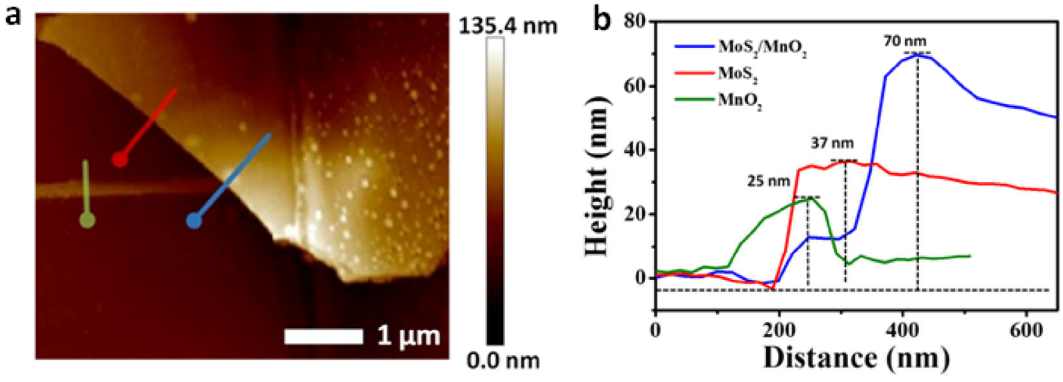

Figure S3 (a) AFM image of MoS_2/MnO_2 heterostructure; (b) The height profile of MoS_2/MnO_2 heterostructure, few-layer MoS_2, and MnO_2 nanowire.

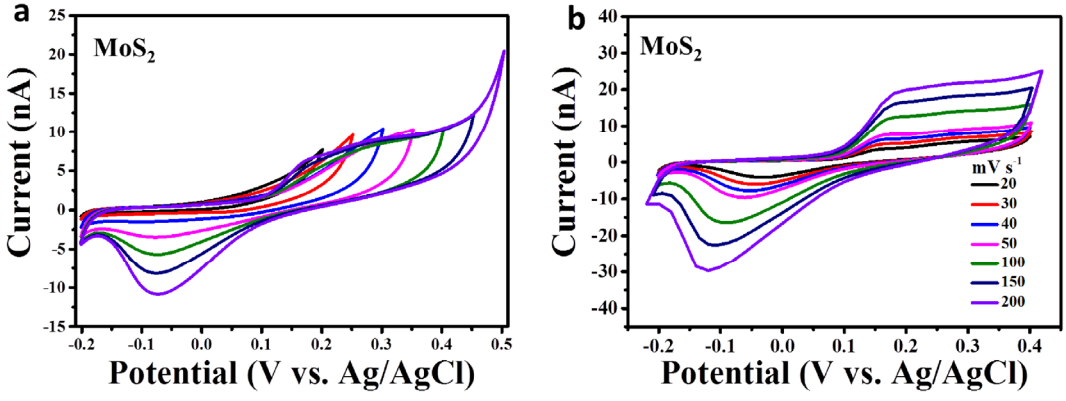

Figure S4 (a) CV curves of multilayer MoS_2 nanosheet at a scan rate of 50 mV s^{-1}. And the CV curves of the electrode materials are tested at different voltage range; (b) CV curves of multilayer MoS_2 nanosheet at different scan rates.

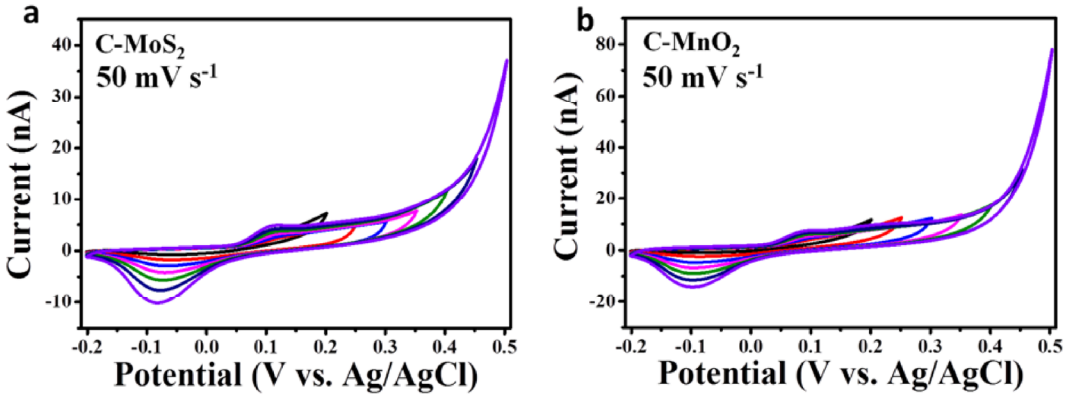

Figure S5 (a) CV curves of MoS_2/MnO_2 heterostructure under C-MoS_2 mode tested at different voltage ranges at a scan rate of 50 mV s^{-1}; (b) CV curves of MoS_2/MnO_2 heterostructure under C-MnO_2 mode tested at different voltages range at a scan rate of 50 mV s^{-1}.

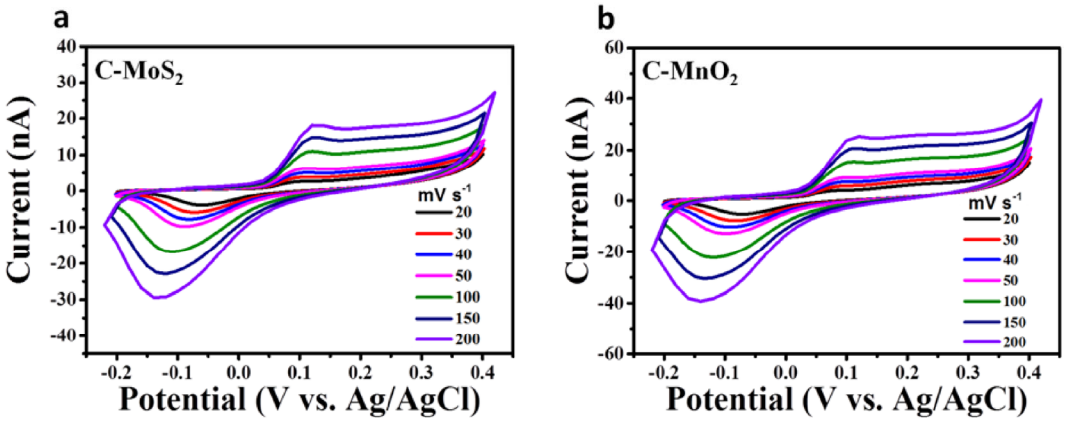

Figure S6 (a) CV curves of MoS_2/MnO_2 heterostructure under C-MoS_2 mode tested at different scan rates; (b) CV curves of MoS_2/MnO_2 heterostructure under C-MnO_2 mode tested at different scan rates.

The electrochemical performances of the energy storage devices were investigated by combining the probe station with the electrochemical workstation. The CV curves of the multilayer MoS_2 nanosheet and MoS_2/MnO_2 heterostructure energy storage devices with different scan rates and voltage window are shown in Figure S4-6 respectively. It can be found that the redox peaks of the MoS_2 appear at 0.15 and -0.04 V respectively. Meanwhile, there is obvious hydrogen evolution reaction in both MoS_2 nanosheet and MoS_2/MnO_2 heterostructure when expanding the voltage window from -0.2 – 0.4 V to -0.2 – 0.5 V. (Figure S4, S5) Thus, a suitable electrochemical voltage window of -0.2 – 0.4 V is chosen for the further measurement.

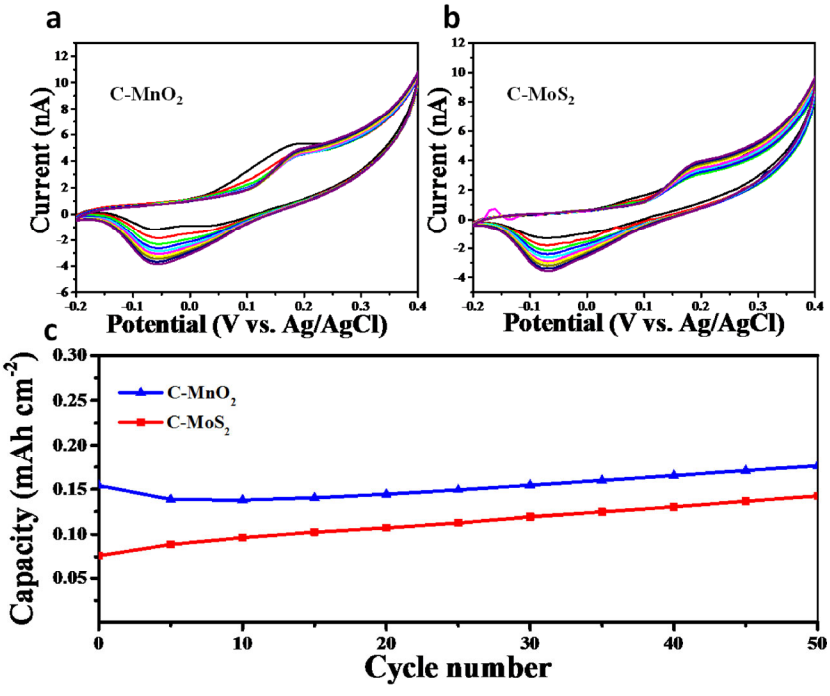

Figure S7 (a) CV curves of MoS_2/MnO_2 heterostructure under C-MnO_2 mode tested at a scan rate of 100 mV s^{-1}; (b) CV curves of MoS_2/MnO_2 heterostructure under C-MoS_2 mode tested at a scan rate of 100 mV s^{-1}; (c) Cycling performances of the MoS_2/MnO_2 heterostructure under C-MnO_2 and C-MoS_2 modes.

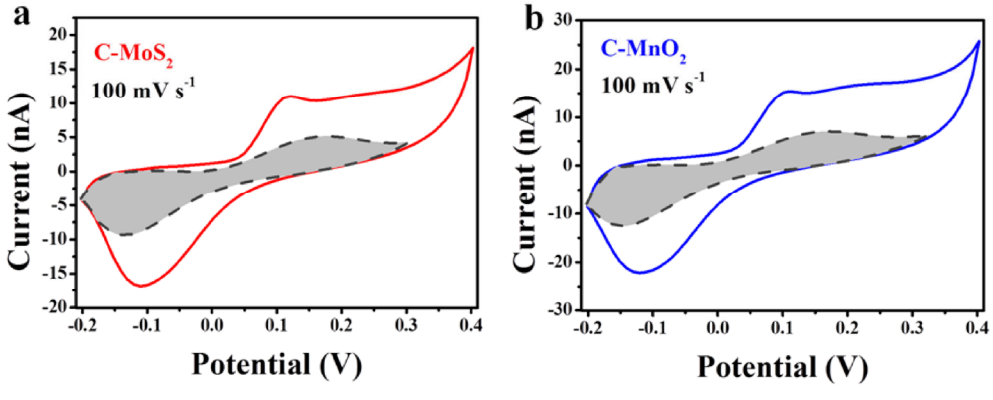

Figure S8 (a) The voltage profile for the surface capacity current (shaded region) is compared with the total measured current obtained at a scan rate of 100 mV s^{-1} for the MoS_2/MnO_2 heterostructure under C-MoS_2 mode; (b) The voltage profile for the surface capacity current (shaded region) compared with total measured current obtained at a scan rate of 100 mV s^{-1} for the MoS_2/MnO_2 heterostructure under C-MnO_2 mode.